RSC Advances

Accepted Manuscript

This article can be cited before page numbers have been issued, to do this please use: U. P. Singh, H. R. Bhat, A. Verma, M. K. Kumawat, R. Kaur, S. K. Gupta and R. K. Singh, *RSC Adv.*, 2013, DOI: 10.1039/C3RA41604F.

Dynamic Article Links ►
View Article Online
DOI: 10.1039/C3RA41604F

Cite this: DOI: 10.1039/c0xx00000x

www.rsc.org/xxxxxx

PAPER

Phenyl hydrazone bearing pyrazole and pyrimidine scaffolds: Design and discovery of novel class of Non-Nucleoside Reverse Transcriptase Inhibitors (NNRTIs) against HIV-1 and their antibacterial properties

Udaya Pratap Singh,*[a,d] Hans Raj Bhat,[a] Amita Verma,[a] Mukesh Kumar Kumawat,[b] Rajinder Kaur,[c] S. K. Gupta[c] and Ramendra K. Singh*[d]

Received (in XXX, XXX) Xth XXXXXXXXX 20XX, Accepted Xth XXXXXXXXX 20XX
DOI: 10.1039/b000000x

Abstract

A novel series of phenyl hydrazone bearing pyrazole and pyrimidine hybrid compounds has been designed using molinspiration toolkit on the basis of Lipinski's rule of five and developed via sequential reactions starting from diazotization of different anilines and further active methylation with acetyl acetone, ethyl acetoacetate and ethyl cynoacetate to generate hydrazono derivatives. The target hybrid compounds have been synthesized on cyclisation of resulting hydrazono derivatives with hydrazine, phenyl hydrazine and urea. These molecules have been subsequently tested for anti-HIV activity using TZM-*bl* cell lines. The MTT assay was also carried out for cytotoxicity determination of active compounds. Further, to exemplify key structural features of the molecules, a molecular docking analysis of most active compound was performed at NNIBP of HIV-RT protein. The antibacterial activity of target compounds was also determined against a panel of four Gram-positive and four Gram-negative human pathogens. All molecules showed potent anti-HIV activity along with prominent inhibition of bacterial organisms.

View Article Online
DOI: 10.1039/C3RA41604F

Introduction

Human immunodeficiency virus (HIV), the causative agent of acquired immune deficiency syndrome (AIDS), causes specific damage to the immune system of the humans both in industrialised and resource poor countries [1]. Despite the decline in number of people newly infected worldwide, HIV is still considered as one of the top three causes of morbidity and mortality. Globally, 34.0 million people were living with HIV at the end of 2011 [2]. For the treatment of HIV, at some point between clinical latency and progression to AIDS, antiretroviral (ARV) therapy is introduced. A highly active antiretroviral therapy (HAART) or triple therapy, presently used for treatment, it includes two nucleoside reverse transcriptase inhibitors (NRTIs) and one additional agent, such as protease inhibitor (PI), non-nucleoside reverse transcriptase inhibitor (NNRTI), or integrase strand transfer inhibitor, as initial ARV regimens for treatment-naïve patients. This combination therapy is extremely effective at lowering viral load and increasing CD4+ T cell levels. However, there has been some debate as to the ideal point for introduction of HAART, and therefore World Health Organisation (WHO) had changed their recommendation from commencement of ARV treatment at a CD4+ T cell count of 200 cells mm^{-3} or below to commencement at 350 cells mm^{-3} in 2010 as this results in considerably better health outcomes [3].

HIV-1 Reverse transcriptase (RT), an enzyme encoded by the viral genome plays an essential role in the replication of HIV catalysing the transcription of viral RNA into viral double-stranded DNA [4]. It is a heterodimeric structure consisting of p66 and p51 subunits, where the p66 subunit is the larger of the two and contains both NRTI and NNRTI binding sites. The p66 subunit consists of RNA- and DNA-dependent DNA polymerase and ribonuclease H (RNase H) domains, both of which are vital for the process of converting single-stranded RNA into double-stranded DNA. The p51 subunit, on the other hand, plays a structural rather than catalytic role, although the protein sequence is identical to that of p66 except that it excludes the RNase H domain [5]. There are two classes of reverse

View Article Online
DOI: 10.1039/C3RA41604F

transcriptase (RT) inhibitors used clinically, namely, nucleoside and non-nucleoside reverse transcriptase inhibitors, NRTIs and NNRTIs, respectively, each affecting the RT enzyme at a different location [6]. NNRTIs serve as more advantageous than NRTIs owing to their unique antiviral activity, high specificity, low toxicity and being independent of host cell metabolism to be converted into an active form [7]. There are about 50 structurally different classes of small hydrophobic molecule targeted at a specific allosteric binding site (an especially flexible pocket formed upon binding of the inhibitor) situated about 10 Å from the polymerase catalytic site and 60 Å from the RNase H active site within the HIV-1 RT. As a result, stimulation of conformational changes at the substrate binding site due to the binding of a non-competitive inhibitor (NNRTI) in the allosteric site substantially reduces the rate of incorporation of nucleotides, thereby halting DNA synthesis. Although they are structurally quite diverse, all NNRTIs bind in the NNRTI binding pocket (NNIBP) in a similar conformation and in identical fashion [8].

Consequently, the wide chemical opportunity due to flexibility of the NNIBP in RT and no mammalian homology of this enzyme (HIV-1 RT) exists, it is considered as a preferred option for the discovery and development of selective newer small molecules. Yet, the main issue in NNRTI drug design is incorporation of the inherent flexibility of the NNIBP, which is surrounded by five aromatic (Tyr-181, Tyr-188, Phe-227 and Trp-229), six hydrophobic (Pro-59, Leu-100, Val-106, Val-179, Leu-234 and Pro-236) and five hydrophilic (Lys-101, Lys-103, Ser-105, Asp-132 and Glu-224) amino acids and thereby creating chances for π–π interactions and hydrogen bonding between the putative inhibitor and the amino acid side chains, Fig. 1 [9]. Despite the innovative drug discovery initiatives, the high cost associated with the HAART therapy also prevents availability of drug regimes in resource poor countries, for instance in South Africa government-funded antiretrovirals are made available at a CD4+ T cell count of 200 cells mm^{-3} or below, unless there is a tuberculosis co-infection or pregnancy [10].

View Article Online
DOI: 10.1039/C3RA41604F

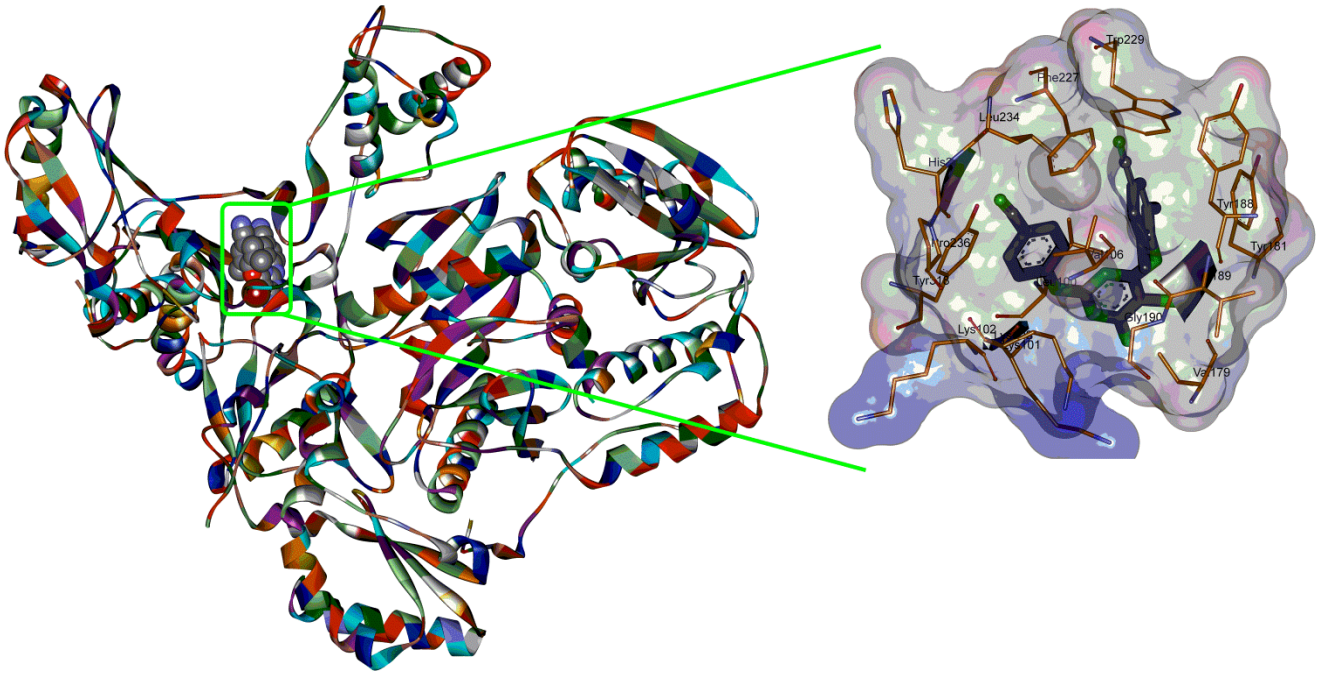

Figure 1: HIV-1 RT heterodimer showing Etravirine (TMC-125) bound in the allosteric site (PDB structures 3m8p).

The design and development of novel heterocyclic core scaffolds that fulfil the pharmacophoric requirement of NNIBP and have cost effective synthesis could be an option worth considering. Pyrazole, pyrimidine and hydrazone are notable heterocyclic scaffolds found to possess wide array of pharmacological activities including anti-HIV [11] and antibacterial activity [12]. In continuation of our ongoing efforts in the discovery of economic NNRTI agents, herein [13], we wish to report a novel class of phenyl hydrazone bearing pyrazoles and pyrimidines in order to obtain more effective candidates. These molecules were designed as per the pharmacophoric requirement to bind efficiently with NNIBP, wherein pyrazole and pyrimidine rings act as pharmacophore and are able to create π-π interaction with amino acid residues present in NNIBP.

The people living with HIV/AIDS (PLWHA) also face serious health threats from "opportunistic" infections (OIs). These infections are called "opportunistic" because they take advantage of weakened immune system and cause devastating illnesses. According to Centre for Disease Control (CDC), more than 20 OIs are considered as AIDS-defining conditions, which include

View Article Online
DOI: 10.1039/C3RA41604F

various bacterial, protozoal and fungal infections [14]. Conversely, the infections caused by bacteria are now recognized with increased prevalence and altered expression in patients with HIV infection. It has been shown to cause substantially increased morbidity and mortality in both early and late stages of HIV infection. As a result, anti-HIV agents possess antibacterial activity, can be able to cure the OIs too and thereby radically improve the situation of PLWHA. Accordingly, designed molecules were also tested for antibacterial activity against three Gram-positive and five Gram-negative human disease causing pathogens.

Results and discussion

Design of compounds

The target compounds were designed using the Molinspiration java based web-applet following Lipinski's rule of five (Ro5) [15]. It is web based software used to obtain parameters such as MiLogP, TPSA and drug likeness. MiLogP (octanol/water partition coefficient) is calculated by the methodology developed by Molinspiration as a sum of fragment-based contributions and correction factors. The method is very robust and is able to process practically all organic and most organometallic molecules. Topological Polar Surface Area (TPSA) is calculated based on the methodology published by Ertl *et al.* as a sum of fragment-based contributions in which O- and N-centered polar fragments are to be considered and calculated by surface areas that are occupied by oxygen and nitrogen atoms and by hydrogen atoms attached to them [16]. TPSA has been shown to be a very good descriptor characterizing drug absorption, including intestinal absorption, bioavailability, Caco-2 permeability and blood brain barrier penetration. Thus, the TPSA is closely related to the hydrogen bonding potential of a compound. The number of Rotatable Bonds – nrotb is a simple topological parameter, which measures the molecular flexibility. It has been shown to be a very good descriptor of oral bioavailability of drugs [17]. It is defined as any single non-ring bond, bound to nonterminal heavy (i.e., non-hydrogen) atom. However, amide C-N bonds are not considered because

View Article Online
DOI: 10.1039/C3RA41604F

of their high rotational energy barrier. Predicted results of target compounds in terms of molecular properties (molecular weight, MilogP and TPSA) are listed in Table 1. The entire set of designed compounds, except 6b, showed no violations from the Lipinski's Ro5, meaning hereby that all molecules fulfilled the optimal requirement for drug absorption.

Table 1: Molinspiration data of the designed compounds

Compounds	miLogP	TPSA	natoms	MW	nON	nOHNH	nviolations	nrotb	volume
6a	4.308	86.154	24.0	323.356	7	0	0	4	289.87
6b	5.158	40.33	22.0	357.255	4	0	1	3	284.421
7a	1.667	113.07	20.0	273.252	8	1	0	3	230.825
7b	2.517	67.246	18.0	307.151	5	1	0	2	225.376
8a	1.338	115.969	18.0	247.214	8	2	0	3	203.406
8b	2.188	70.145	16.0	281.113	5	2	0	2	197.957
9a	2.68	105.112	24.0	323.312	8	1	0	4	275.196
9b	3.53	59.288	22.0	357.211	5	1	0	3	269.747
10a	0.723	141.992	18.0	248.202	9	4	0	3	198.134
10b	1.573	96.168	16.0	282.101	6	4	0	2	192.685
10c	1.418	96.168	16.0	237.65	6	4	0	2	188.335
10d	1.442	96.168	16.0	237.65	6	4	0	2	188.335
11a	2.065	131.135	24.0	324.3	9	3	0	4	269.924
11b	2.915	85.311	22.0	358.199	6	3	0	3	264.475
11c	2.76	85.311	22.0	313.748	6	3	0	3	260.125
11d	2.784	85.311	22.0	313.748	6	3	0	3	260.125

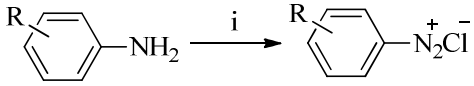

1a, R= 4-NO_2 **2a, R**= 4-NO_2
1b, R= 4-Br **2b, R**= 4-Br
1c, R= 3-Cl **2c, R**= 3-Cl
1d, R= 4Cl **2d, R**= 4Cl

Scheme 1: Diazotization of anilines. Reagents and conditions: (i) $NaNO_2$/HCl, stirring, 1h.

View Article Online
DOI: 10.1039/C3RA41604F

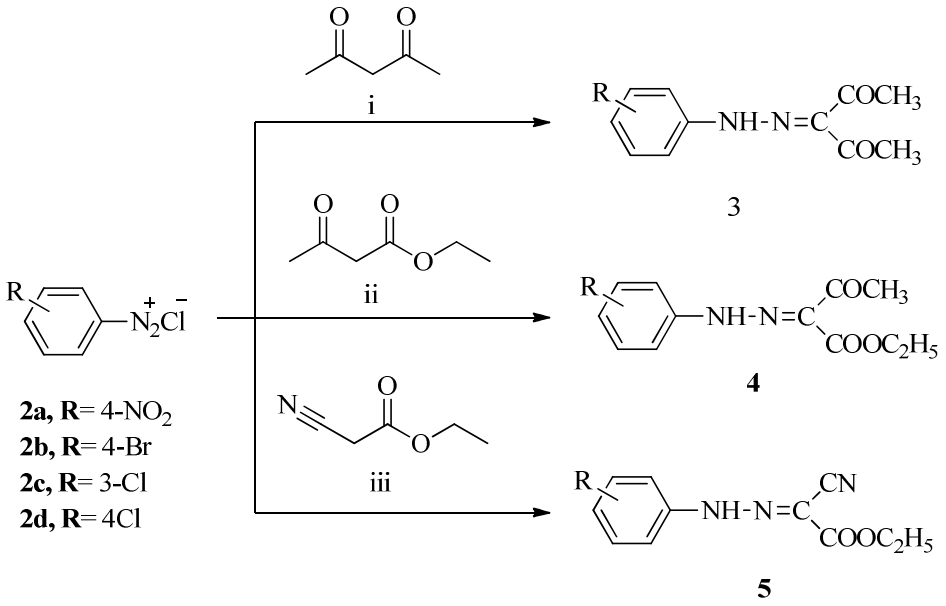

Scheme 2: Synthesis of hydrazono derivatives via active methylene compounds. Reagents and conditions: Stirring 3h

View Article Online
DOI: 10.1039/C3RA41604F

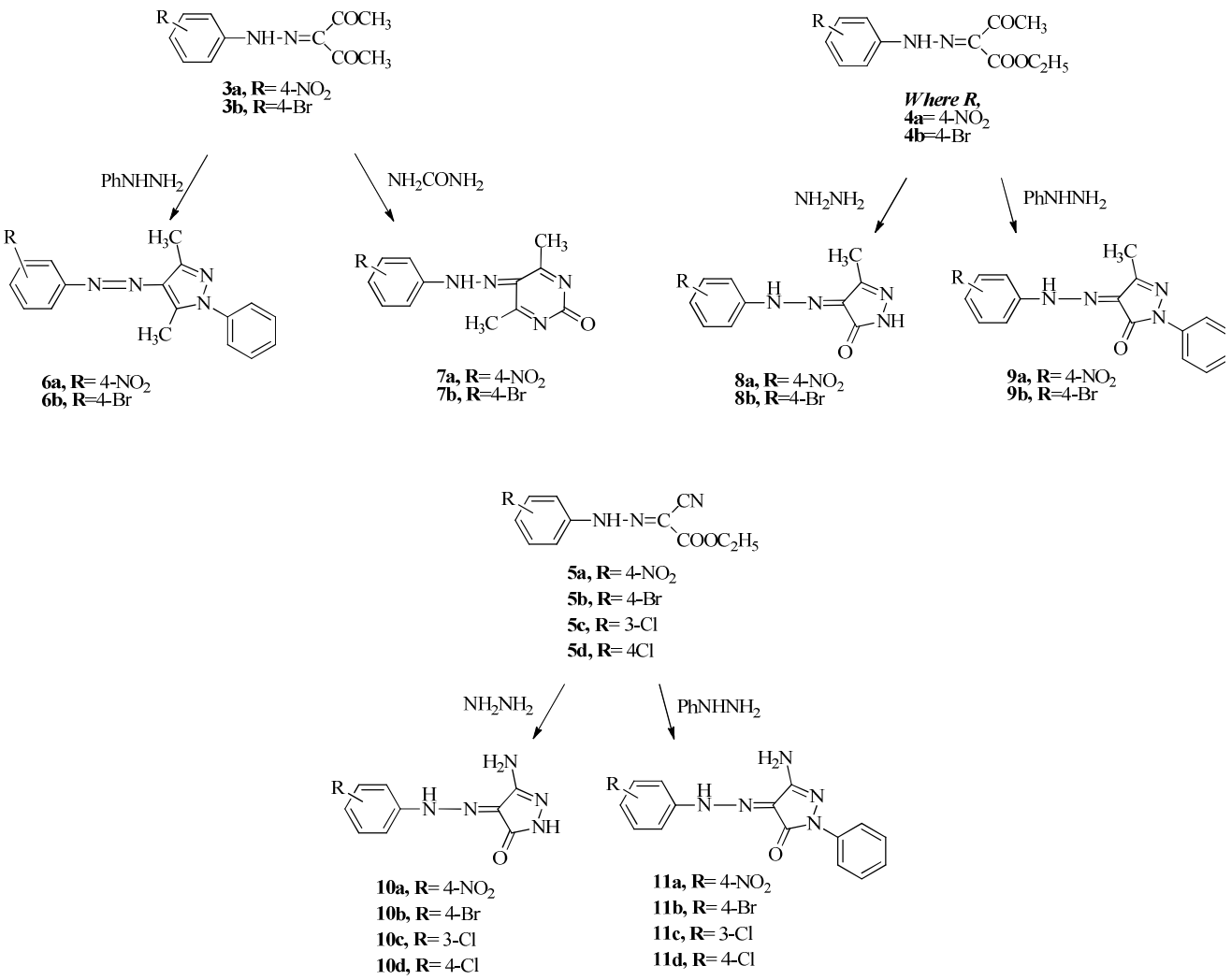

Scheme 3: Synthesis of target compounds via cyclization of hydrazono derivatives using hydrazine, urea and phenyl hydrazine

View Article Online
DOI: 10.1039/C3RA41604F

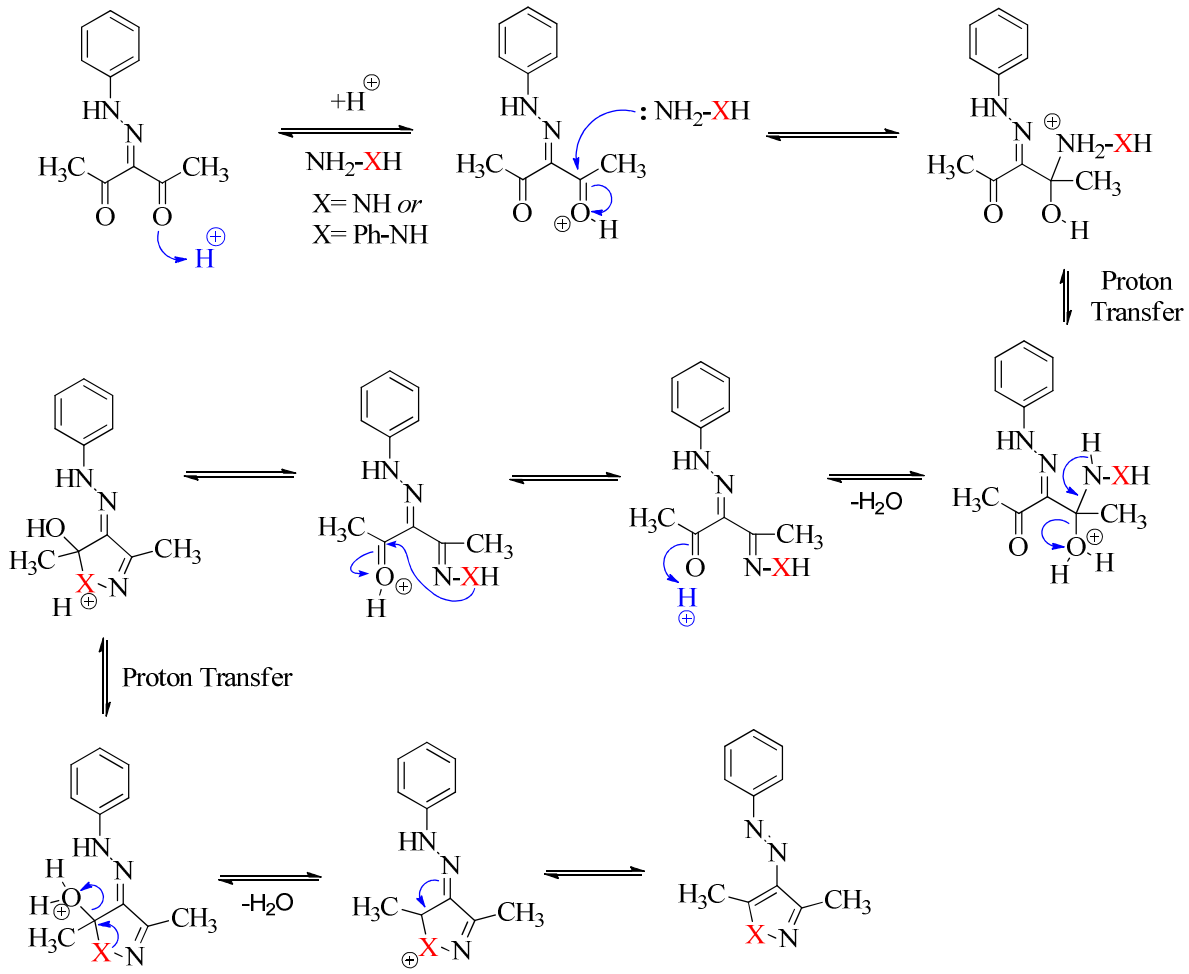

Figure 2: Proposed mechanism of pyrazole ring synthesis

View Article Online
DOI: 10.1039/C3RA41604F

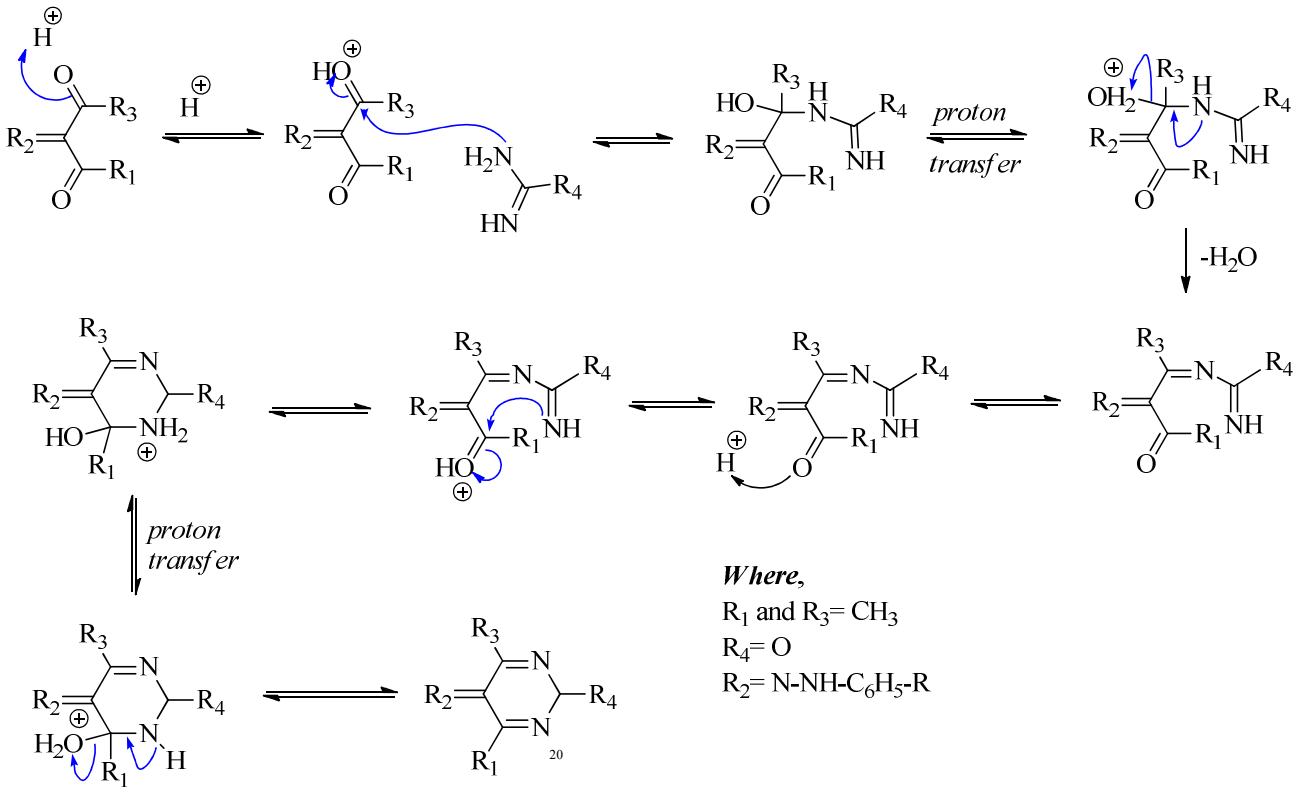

Figure 3: Proposed mechanism of pyrimidine ring synthesis

Chemistry

The synthesis of target compounds *viz.* pyrazole and pyrimidine derivatives was achieved as shown in Scheme 1-3 and the mechanism of pyrazole and pyrimidine ring generation in fig. 1 and 2. The synthesis was initiated with the formation of diazonium chlorides of respective anilines **2**(**a-d**) upon diazotization of **1**(**a-d**) using a mixture of sodium nitrite and concentrated HCl at 0-5 □C. Diazonium salts thus obtained were treated with calculated amounts of ice-cold active methylene compounds, namely acetyl acetone, ethyl acetoacetate, ethyl cynoacetate in the presence of sodium acetate to afford hydrazono derivatives 3, 4 and 5, respectively. These hydrazono derivatives further underwent cyclization with hydrazine or phenyl hydrazine in boiling ethanol to the corresponding

View Article Online
DOI: 10.1039/C3RA41604F

pyrazolin-5-one derivatives of substituted anilines, compound **8**(**a**,**b**) and **9**(**a**,**b**). The structures of these newly formed derivatives were ascertained by IR, ^{1}H NMR, ^{13}C NMR and elemental analysis. The IR spectra showed the disappearance of the characteristic bands of acetyl carbonyl group and carboxylic acid ester and appearance of strong bands in the 3107-3211 cm^{-1} region, attributable to NH stretching. The bands of pyrazolinone ring υ C=O groups appeared in the range of 1662-1676 cm^{-1}. The ^{1}H-NMR spectra of compounds **8**(**a**,**b**) and **9**(**a**,**b**) showed the presence of CH_3 signal at δ 2.31-2.51 ppm. The ^{13}C NMR of **8b**, for example, confirmed the absence of acetyl C=O and carboxylic acid ester groups and appearance of two methyl signal in the high field region. The other carbon atoms of pyrazolinone and phenyl moieties all appeared at the expected chemical shift. The compounds **10**(**a-d**) and **11**(**a-d**) were synthesized via cyclization of **5**(**a**,**b**) with hydrazine and phenyl hydrazine (Scheme 3). The IR spectra of **10**(**a-d**) and **11**(**a-d**), were characterized by the disappearance of υ CN band and the appearance of band at 3217-3385 cm^{-1} attributable to the stretching vibration of the υ NH_2 group. Diagnostically, a singlet at 5.61 ppm in the ^{1}H NMR spectrum of **10b** was attributable to the NH_2 proton.

3,5-Dimethyl-4-((4-nitrophenyl)diazenyl)-1-phenyl-4,5-dihydro-1*H*-pyrazole (**6a**) and its bromo derivative **6b** were obtained by thermal cyclization of **3**(**a**,**b**) with phenyl hydarazine in glacial acetic acid (Scheme 3). The IR spectra of **6**(**a**,**b**) were characterised by disappearance of υ NH and acetyl group C=O absorption bands and bands at 1455, 1445 cm^{-1} indicated the presence of N=N. The ^{1}H NMR spectra of **6**(**a**,**b**) showed the presence of two methyl groups and the aromatic protons all appeared at expected chemical shift. The reaction of hydrazono derivative **3**(**a**,**b**) with urea in ethanol under reflux for 5h gave solid products **7**(**a**,**b**). Compound **7a** displayed bands in IR spectrum at 3118 (NH) and 1680 (pyrimidine-2-one C=O) cm^{-1}. Structure of **7a**, was confirmed by ^{13}C-NMR spectra, which provided conclusive evidence for the formation of pyrimidin-2-one structure by showing singlet at 196.60, 195.12, 166.16 and 139.65.

View Article Online
DOI: 10.1039/C3RA41604F

Anti-HIV activity

Initially ten compounds from the target dataset, *viz*. **8a**, **8b**, **9a**, **9b**, **10a**, **10b**, **10c**, **11a**, **11b** and **11c** were selected on the basis of *in silico* study to determine the possible anti-HIV activity against the TZM-*bl* cells at the concentration of 50 μg mL^{-1}. The results are presented in Table 2. It was observed that compounds **8a**, **8b**, **10a** and **10c** showed more than 85 % inhibition of HIV at a test dose with maximum 98 % in the case of compound **10b**. Out of these, six compounds showed more than 40 % inhibition were subsequently subjected to cytotoxicity determination using MTT assay (Table 3). It has been observed that the increase in concentration of compounds **8a**, **8b**, **10(a-c)** from 25 μg mL^{-1} to 125 μg mL^{-1} (five-fold increase) does not appreciably lower the percentage of cell viability. Hence, it was inferred that, molecules showed potent anti-HIV activity, while presenting no significant toxicity at test dosages under *in vitro* conditions.

Table 2 Anti-HIV activity of the selected compounds

Compound	Concentration (in μg mL^{-1})	Percentage of Inhibition
8a	50	85
8b	50	91
9a	50	0
9b	50	10
10a	50	91
10b	50	98
10c	50	93
11a	50	41
11b	50	20
11c	50	0

Table 3 Cytotoxicity assay of the compounds†

Compound	125 μg mL^{-1}	25 μg mL^{-1}	5 μg mL^{-1}	1 μg mL^{-1}	0.2 μg mL^{-1}
8a	31	34	87	82	90
8b	27	26	32	96	102
10a	33	32	81	80	89
10b	27	28	44	40	70
10c	20	25	40	52	67
11a	40	49	84	86	90

†: Results presented as percentage of cell viability

View Article Online
DOI: 10.1039/C3RA41604F

Molecular docking

It is a significant computational method used to forecast the binding of the ligand to the receptor binding site. The molecules **8b** and **10b** were docked within NNIBP of HIV-RT to assess their mode of interaction and structural requirement for HIV-1 RT inhibition (Table 4). The formation of one hydrogen bond was revealed between HIV-1 RT Leu234 and pyrazole N on inspecting the post-dock pose of compound 8b at NNIBP inside the HIV-1 RT protein (Fig. 5). It was fashioned via Leu234 with the involvement of hydrogen of pyrazole nitrogen as shown in Fig. 4, Table 4. Further, formation one of π- π and σ- π interactions with Tyr318 and Val106, respectively via phramacophoric pyrazole nuclei was also observed. In another highly active molecule, **10b**, the pyrazole ring was oriented as face-to-face with HIV-1 RT Tyr181 creating π-π stacking interaction, while showing the formation of one hydrogen bond via hydrazone with Tyr188.

A close inspection of best docked pose of compound **10b**, clearly establish that it attained a "horseshoe-like conformation as that of second generation NNRTIs and similar interaction with Tyr181 and Tyr188 of p66 subunit in the NNIBP, Fig 5 [18]. The compound 8b, however, did no show similar orientation. Therefore, on the basis of conformational analysis of post-docked poses of ligands **8b** and **10b**, it was inferred that higher activity of compound **10b** was attributable to its conformational flexibility within the NNIBP.

Further, these molecules were evaluated by a scoring function to distinguish between good (near native) and bad (decoy) docking solutions. Scoring functions for molecular docking are traditionally either physics-based or knowledge-based and differ mainly in the derivation of the mathematical models. It is very vital as it used to compute the strength of the non-covalent interaction, called as binding affinity, between two molecules after they have been docked. To define binding affinity of ligands with receptor in a better way, docked compounds (**8b** and **10b**) were rigorously analysed through scoring function as shown in Table 5.

View Article Online
DOI: 10.1039/C3RA41604F

The affinity of the molecules against the receptor was initially determined by LUDI3 score. It is a *de novo* ligand design program that reckons interaction sites with a receptor and suggests small molecular fragments that are able to interact with the receptor. This program analyses a geometrical fit of given chemicals into the binding site and calculates other determinants of good binding, such as hydrogen bonds, lipophilic interactions, ionic interactions, and acylic interactions [19]. In general, a higher *Ludi* score represents higher affinity and stronger binding of a ligand to the receptor, as is shown in the case of **10b** (510, most active) than **8b** (460, less active).

Piecewise Linear Potential is a fast and simple docking function that has been shown to elucidate the protein ligand binding affinities in an efficient way. The PLP scores are measured in arbitrary units and higher PLP scores indicate stronger receptor-ligand binding. Two versions of the PLP function are available and used in the present case: PLP1 [20] and PLP2 [21]. In the PLP1 function, each non-hydrogen ligand or non-hydrogen receptor atom is assigned a PLP atom type. Hydrogen atoms are excluded from consideration. Whereas, in PLP2 function, PLP atom typing remains the same as in PLP1. In addition, an atomic radius is assigned to each atom except for hydrogen. It is worthwhile to mention that the most active compound (**10b**) was also found in conformity of PLP scoring functions, showing higher values than corresponding less active molecule, **8b**.

The PMF scoring functions were developed on the basis of statistical analysis of the 3D structures of protein-ligand complexes. These were found to correlate well with protein-ligand binding free energies. The scores are calculated by summing pairwise interaction terms over all interatomic pairs of the receptor-ligand complex [22]. Again, compound **10b** being highly active, prevailed over **8b** in terms of PMF scoring, proving the experimental results.

The internal non-bonded ligand energy is calculated for each new conformation that is generated. Bad conformations with high internal ligand energies (typically resulting from internal close contacts) are discarded. The internal ligand energy consists of a van der Waals (vdW) term and an optional electrostatic term. The non-bonded vdW energy is computed using a standard 9-6 (unsoftened)

View Article Online
DOI: 10.1039/C3RA41604F

potential using forcefield parameters consistent with the forcefield employed. Readings revealed **10b** as an efficient ligand owing to its high negative ligand internal energy than compound **8b**.

Additionally, these molecules were analysed using Lig score and dock score, which classified as empirical and knowledge based scoring functions, respectively [23]. The most active molecule, **10b**, presented higher values than corresponding less active molecule **8b**, which in generalized manner, held true for highly active ligands.

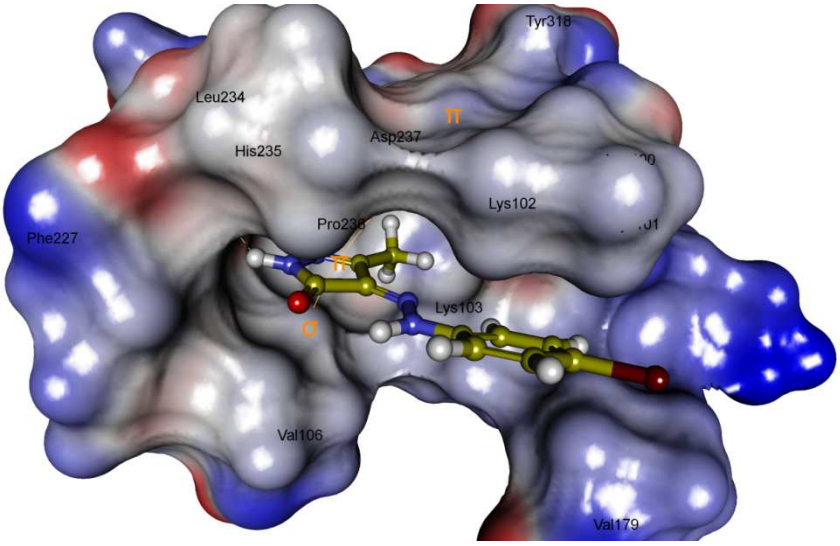

Figure 4 Post-docked conformation of ligand **8b** in complex with the HIV-1 RT at NNIBP

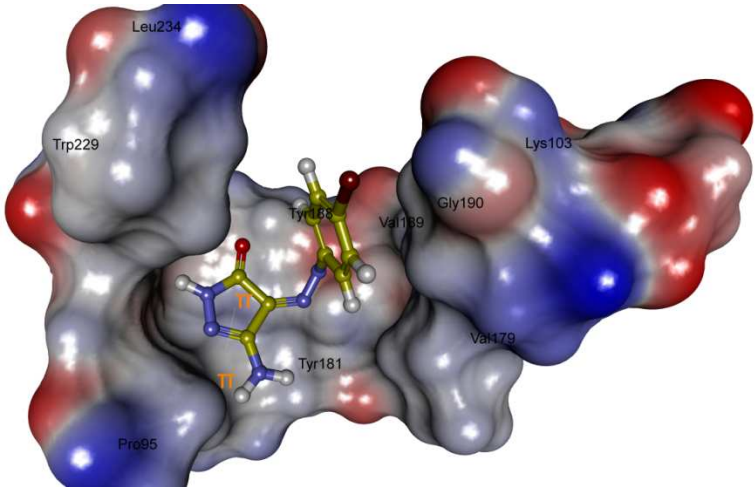

Figure 5 Post-docked conformation of ligand **10b** in complex with the HIV-1 RT at NNIBP

View Article Online
DOI: 10.1039/C3RA41604F

Table 4 Interaction of compound **8b** and **10b** in the NNIBP of HIV-1 RT protein structure

Compound	3m8p.pdb		
	Hydrogen bond	Pi-pi	Pi-Sigma
8b	Amine NH…..Leu234	Pyrazole-Tyr318	Pyrazole—Val106
10b	Hydrazone, N…Tyr188	Pyrazole-Tyr181	NO

Table 5 Docking scores of compound **8b** and **10b**

S. No	Scoring parameter	8b	10b
1	Ludi3	460	510
2	-PLP1	59.41	68.51
3	-PLP2	58.21	63.78
4	-PMF	14.67	59.62
5	Jain	1.52	2.85
6	Lig Internal energy	-1.79	-1.54
7	Lig Score 1 Dreiding	2.16	2.61
8	Lig score2 Dreiding	4.34	4.86
9	Dock Score	38.98	39.24
10	Binding Energy (in kcal mol^{-1})	-51.54	-33.53

Antibacterial activity

All synthesized compounds were screened for their minimum inhibitory concentration (MIC, µg/mL) against a panel of four Gram-positive, *viz. Staphylococcus aureus* (NCIM-2079), *Bacillus subtilis* (NCIM-2063), *Bacillus cereus* (NCIM-2156), *Staphylococcus Epidermidis* and four Gram-negative bacterial strains *viz. Pseudomonas aeruginosa* (NCIM-2036), *Escherichia coli* (NCIM-2065), *Proteus Mirabilis* and *Proteus vulgaris* for determination of their antibacterial efficacy using cefixime as a standard drug and results were presented in Table 6. It is noteworthy to mention here that the entire set of test compounds showed marked to considerable inhibition pattern against the bacterial strains and even some cases showed more potent activity than the reference standard. From table 6, it was inferred that compound **6a** showed more potent activity against *B. cereus* and *B. subtilis*, equi-

View Article Online
DOI: 10.1039/C3RA41604F

potent to *S. aureus*, *P. aeruginosa* and *E. coli* in comparison to cefixime and considerable to least activity against rest of the strains. Introduction of halogen atom (**6b**, bromo) in the place of nitro group causes drastic reduction in activity against *P. aeruginosa* and *E. coli*. On the contrary, in comparison to the standard, it showed marked increase in activity against *S. epidermidis* and potent in the case of rest of the strains. On substituting the pyrazole with di-methyl pyrimidine, **7a**, having nitro group on phenyl hydrazone showed moderate to less activity against *B. cereus*, *P. aeruginosa*, *E. coli*, *S. epidermidis* and *B. subtilis*, it showed considerably potent activity against *S. aureus*, *P. mirabilis*, and equipotent to *P. vulgaris* in comparison to standard. A significant shift in antibacterial profile was observed on replacing nitro group with bromo resulting in potent to significant activity against entire range of bacterial strains. Notably, mild to no activity was observed against all the three Gram positive strains by compound **8a** except *S. epidermidis*. Additionally, this compound showed more potent activity against *P. mirabilis* and *P. vulgaris* in comparison to standard. However, not very significant difference in activity was witnessed on insertion of bromo in the place of nitro group, while a presence of extra phenyl on the pyrazole revealed prominent inhibition pattern ranging from potent to considerable activity on the entire set of tested microorganisms. The compound **10a** showed potent activity against *P. mirabilis* and considerable to less activity against rest of the test strains. However, equi-potent activity was disclosed in the case of Gram-positive microorganisms and *P. aeruginosa* and showed much significant activity against rest of the strains on substituting nitro with bromo group. A substantial loss in activity was observed on introduction of 3-chloro at the phenyl of hydrazone, **10c**, against entire set of the bacterial strains except significantly potent activity against *S. aureus*, *E. coli* and *P. mirabilis*. To our surprise, drastic upsurge in activity of **10d** was reported against entire bacterial strains and showed the compound potent in majority of cases except *P. vulgaris* and *E. epidermidis* on isomeric replacement of chloro from second to fourth position. Moderate to least activity was disclosed by compound **11a** against *S. aureus*, *P aeruginosa* and *S. epidermidis*. However, it also showed equipotent activity against *B. subtilis*, *B. cereus* and *P. vulgaris*; and significant to more

View Article Online
DOI: 10.1039/C3RA41604F

potent activity against rest of the microorganisms. Conversely, significant increase in potency and inhibitory activity of compound **11b** was reported against entire panel of tested bacterial strains except *S. epidermidis* on introduction of bromo into the core structure. The drastic decline in activity was reported by compound **11d** against majority of strains except *S. epidermidis*, which showed better inhibition pattern. Additionally, no major noticeable change in activity profile was reported by **11d**, an isomeric counterpart of **11c**, compound **11d**.

On the basis of antibacterial spectrum of the tested compounds, structure-activity relationship (SAR) studies suggested that activity was radically improved by the presence of halogen atom and was further substantiated by presence of additional phenyl ring on the heterocyclic core. The ease of penetration into the bacteria via altering the integrity of cell wall due to the presence of electron withdrawing group may be the plausible factor to switch the potency of the compound, which is further found in agreement with the corresponding physico-chemical parameter discussed in Table 1. Moreover, presence of additional phenyl ring makes the compound more lipophilic and enhances antibacterial activity via increasing the permeability of the compounds across the cell wall, for instance, **6a**, **6b**, **9a**, **9b** and **11**(**a-d**). It was also revealed that presence of methyl group at R_1 as shown in Fig. 6, made the molecules more active towards both the tested strains, while activity abolishes on introduction of basic NH_2 group. The presence of CH_3 along with other CH_3 of pyrazole enhances the activity, suggesting the role of di-methyl pyrazole, while drastic reduction in activity was observed on introduction of >C=O group at R_2 position against Gram-positive strains along with no significant change against Gram-negative organisms, Fig. 6. Moreover, replacement of pyrazole with pyrimidine nuclei resulted in marginal loss of activity. On closely inspecting the Table 1, the factors like TPSA, molecular weight and volume of the entire compounds were found in optimal range and contributed towards the better absorption and considerable bio-activity. A significant change in activity was reported by the compounds having *para*-chloro group rather than its isomeric *meta* configuration, *viz*. **10c** and **10d**; **11c** and **11d**.

View Article Online
DOI: 10.1039/C3RA41604F

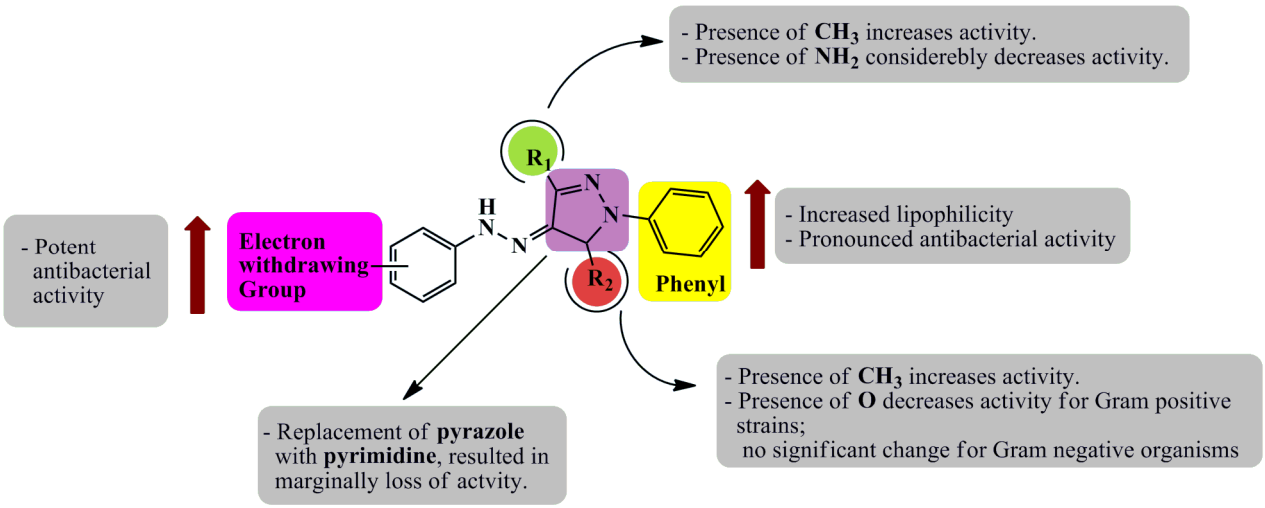

Figure 6: Structure–activity relationship (SAR) of designed target derivatives as antibacterial agent.

Table 6: Antibacterial data of target compounds (presented as MIC in μg mL^{-1}).

Compounds	*S. aureus*	*B. subtilis*	*B. cereus*	*S. Epidermidis*	*P. aeruginosa*	*E. coli*	*P. mirabilis*	*P. vulgaris*
6a	12.5	3.125	1.56	100	3.125	3.125	50	50
6b	3.125	1.56	50	6.25	50	25	12.5	1.56
7a	6.25	100	6.25	50	50	50	1.56	12.5
7b	3.125	3.125	6.25	12.5	1.56	3.125	1.56	12.5
8a	50	100	100	12.5	6.25	12.5	3.125	6.25
8b	25	50	100	12.5	3.125	12.5	6.25	3.125
9a	1.56	3.125	3.125	12.5	1.56	3.125	25	3.125
9b	3.125	6.25	12.5	1.56	3.125	50	12.5	1.56
10a	12.5	12.5	12.5	12.5	6.25	12.5	3.125	3.125
10b	12.5	12.5	6.25	6.25	3.125	6.25	1.56	1.56
10c	6.25	25	25	100	25	3.125	6.25	50
10d	3.125	1.56	25	50	1.56	3.125	3.125	25
11a	50	1.56	6.25	100	50	6.25	6. 25	12.5
11b	3.125	1.56	6.25	50	3.125	6.25	1.56	50
11c	50	50	12.5	6.25	100	50	100	50
11d	50	50	12.5	3.125	50	12.5	100	12.5
Cefixime	12.5	12.5	6.25	6.25	3.125	3.125	12.5	12.5

Experimental

Design of the compounds

Design of the target compounds was done in accordance with Lipinski's rule of 5 (Ro5) using Molinspiration web applet.

View Article Online
DOI: 10.1039/C3RA41604F

Structural Investigation

All chemicals were of analytical grade and used directly. Melting points determined in open capillary tubes with electrothermal melting point apparatus (MP-1) are uncorrected. The completion of reaction was checked by thin layer chromatography (TLC) using silica gel-G coated Al-plates (0.5 mm thickness; Merck) and the plates were illuminated under UV (254 nm) and evaluated in iodine. FT-IR (in 2.0 cm-1, flat, smooth, abex, KBr) spectra were recorded on Perkin Elmer-Spectrum RX-I spectrometer. ^{1}H NMR spectra were recorded on Bruker Avance II 400 NMR Spectrometer and ^{13}C NMR spectra on Bruker Avance II 100 NMR spectrometer in DMSO-d_6 using TMS as the internal standard. Chemical shift is reported in parts per million (ppm, δ), and signals are described as s (singlet), d (doublet), t (triplet), q (quartet), and m (multiplet). Solvents were purified prior to use according to standard protocols.

Diazotization of substituted anilines

A solution of substituted anilines **1**(**a**-**d**) in concentrated HCl (3-4 mL) was cooled to 0-5 □C under ice, and a cold sodium nitrite solution (1.5 g in 10 mL of water) added to it drop-wise during 10 min. The reaction mixture was then stirred for 1h which afforded the desired diazonium salt of respective aniline.

General procedure for the preparation of hydrazono derivatives

To an ice-cold mixture of appropriate active methylene compound [acetyl acetone (i), ethyl acetoacetate (ii), ethyl cyanoacetate (iii)] (0.01 mol) and sodium acetate (0.05 mol) in ethanol (50 mL) was added drop-wise with stirring a solution of diazonium salt compound (0.01 mol) over 20 min. The stirring was continued for 1 h and the reaction mixture was then left for 3 h at room temperature. The solid product was collected and recrystallized from ethanol to give the corresponding hydrazono derivative (**3**, **4** and **5**).

View Article Online
DOI: 10.1039/C3RA41604F

General procedure for cyclisation reactions

Method A: With Hydrazine hydrate

A mixture of appropriate hydrazone (4 a,b and 5 a-d) and hydrazine hydrate (0.01 mol) in ethanol (30 mL) was heated under reflux for 6-8 h. The solvent was concentrated and the reaction product was allowed to cool. The separated product was filtered off, washed with water, dried and recrystallized from ethanol.

3-Methyl-4-(2-(4-nitrophenyl)hydrazono)-1*H*-pyrazol-5(4*H*)-one **8a**

Pale-yellow crystals; Yield: 85 %; M.P.: 240-242 □C; FTIR υ_{max} (in cm^{-1}): 3197.98 (Secondary -NH stretching), 1676.14 (-C=O stretching), 1566.20 (-NH bending), 1527.62 (Asymmetrical, $-NO_2$ stretching), 1433.11 (Symmetrical, $-NO_2$ stretching), 1350.17 (-C=C- stretching, Ar), 1242.16-1203.58 (-C-N stretching), 1070.49-572.86 (-C-H bending, Ar); ^{1}H NMR (400MHz, $CDCl_3$-d_6, TMS) δ ppm: 1.18-1.19 (d, 3H *J*=8 Hz, CH_3), 2.16 (s, 1H, NH, Ar-H), 2.50-2.51 (m, 1H, CH, aliphatic), 7.80-7.83 (d, 1H *J*=12 Hz, Ar-H), 7.88-7.90 (d, 1H *J*=8 Hz, Ar-H), 7.98 (s, 1H, amide); ^{13}C NMR (100MHz, $CDCl_3$) δ ppm: 159.91 (C-amide), 148.63 (C-NH, Ar), 142 (C-NO_2, Ar), 121.23 (CH, Ar), 109.72 (CH, Ar), 78.71 (CH, aliphatic), 40.24 (CH, aliphatic), 11.49 (CH_3). Elemental Analysis for $C_{10}H_9N_5O_3$: C, 48.58, H, 3.67, N, 28.33 (calculated): C, 48.60, H, 3.69, N, 28.30 (found).

4-(2-(4-Bromophenyl)hydrazono)-3-methyl-1*H*-pyrazol-5(4*H*)-one **8b**

Dark-pale yellow crystals; Yield: 81%; M.P.: 220-222 □C; FTIR υ_{max} (in cm^{-1}): 3211.48 (Secondary -NH stretching), 1666.50 (-C=O stretching), 1587.42-1566.20 (-NH bending), 1483.26-1375.25 (-C=C- stretching, Ar), 1249.87 (-C-N stretching), 1070.49 (-C-Br stretching), 968.27-594.08 (-C-H bending, Ar); ^{1}H NMR (400MHz, $CDCl_3$-d_6, TMS) δ ppm: 1.19 (d, 3H *J*=4 Hz, CH_3), 2.13 (s, 1H, NH, aromatic), 2.50 (m, 1H, CH, aliphatic alicyclic), 7.34-7.37 (d, 1H *J*=12 Hz, Ar-H), 7.44-7.48 (d, 1H *J*=16 Hz, Ar-H), 8.01(s, 1H, C-NH, amide); ^{13}C NMR (100MHz, $CDCl_3$) δ ppm: 160.23 (C-amide),

View Article Online
DOI: 10.1039/C3RA41604F

146.64 (C-NH, Ar), 140.58 (CH, Ar), 132.0 (CH, Ar), 128.71 (C-Br, Ar), 78.12 (CH, aliphatic), 38.98 (CH, aliphatic), 11.43 (CH_3, aliphatic); Elemental Analysis for $C_{10}H_9BrN_4O$: C, 42.73, H, 3.23, N, 19.93 (calculated): C, 42.70, H, 3.22, N, 19.93 (found).

3-Amino-4-(2-(4-nitrophenyl)hydrazono)-1*H*-pyrazol-5(4H)-one **10a**

Brown crystals; Yeild: 78%; M.P.: 291-293 □C ; FTIR υ_{max} (in cm^{-1}): 3685.07-3462.22 (Primary -NH stretching), 3197.98 (Secondary -NH stretching), 1674.21 (-C=O stretching), 1624.06 (Primary -NH bending), 1581.63 (Asymmetrical, $-NO_2$ stretching), 1533.41 (Symmetrical, $-NO_2$ stretching), 1354.03 (Secondary -NH bending), 1249.87-1209.37 (-C=C- stretching, Ar), 1109.07 (-C-N stretching), 989.48-682.80 (-C-H bending, Ar); ^{1}H NMR (400MHz, $CDCl_3$-d_6, TMS) δ ppm: 1.05-1.08 (m, 1H, CH, aliphatic), 1.19 (s, 2H, NH_2), 2.50-2.51 (m, 1H, CH, aliphatic), 3.28 (s, 1H, NH, Ar), 7.51-7.55 (t, 1H *J*=16 Hz, Ar-H), 7.77-7.79 (d, 1H *J*=8 Hz, Ar-H), 7.84-7.86 (d, 1H *J*=8 Hz, Ar-H), 7.97 (s, 1H, amide); ^{13}C NMR (100MHz, $CDCl_3$) δ ppm: 158.36 (C-amide), 148.75 (C-NH, Ar), 130.12 (C-NO_2, Ar), 120.95 (CH, Ar), 117.72 (CH, Ar), 78.69 (CH, aliphatic alicyclic), 40.24 (NH_2-CH, aliphatic alicyclic); Elemental Analysis for $C_9H_8N_6O_3$: C, 43.55; H, 3.25; N, 33.86 (calculated): C, 43.58; H, 3.22; N, 33.80 (found).

3-Amino-4-(2-(4-bromophenyl)hydrazono)-1*H*-pyrazol-5(4*H*)-one **10b**

Dark-brown crystals; Yeild: 89 %; M.P.: 265-267 □C; FTIR υ_{max} (in cm^{-1}): 3355.78-3300.20 (Primary -NH stretching), 3188.82 (Secondary -NH stretching), 1641.42 (-C=O stretching), 1598.99 (Primary -NH bending), 1521.48 (Secondary -NH bending), 1485.19-1363.67 (-C=C- stretching, Ar), 1247.94 (-C-N stretching), 1112.93 (-C-Br stretching), 1082.49-572.86 (-C-H bending, Ar); ^{1}H NMR (400MHz, $CDCl_3$-d_6, TMS) δ ppm: 2.50-2.51 (d, 2H *J*=4 Hz, NH_2), 3.49 (m, 1H, CH, aliphatic alicyclic), 4.31 (m, 1H, CH, aliphatic alicyclic), 5.61(s, 1H, NH, Ar-H), 7.40-7.50 (m, 1H, Ar-H), 8.09 (s, 1H, amide); ^{13}C NMR (100MHz, $CDCl_3$) δ ppm: 149.62 (C-amide), 141.10 (CH, Ar), 131.86 (CH, Ar), 116.74

View Article Online
DOI: 10.1039/C3RA41604F

(CH, Ar), 115.87 (C-Br, Ar), 78.92 (CH, aliphatic), 40.21 (CH, aliphatic); Elemental Analysis $C_9H_8BrN_5O$: C, 38.32; H, 2.86; N, 24.83 (calculated): C, 38.35; H, 2.89; N, 24.86 (found).

3-Amino-4-(2-(3-chlorophenyl)hydrazono)-1*H*-pyrazol-5(4H)-one **10c**

Dark-brown crystals: Yeild: 87 %; M.P.: 160-162 □C; FTIR υ_{max} (in cm^{-1}): 3385.07 -3325.28 (Primary -NH stretching), 3186.40 (Secondary -NH stretching), 1683.86 (-C=O stretching), 1637.56-1600.92 (Primary -NH bending), 1481.33 (Secondary -NH bending), 1404.40-1253.73 (-C=C- stretching, Ar), 1207.44(-C-N stretching), 1114.06 (-C-Cl stretching), 999.13-588.57 (-C-H bending, Ar); ^{1}H NMR (400MHz, $CDCl_3$-d_6, TMS) δ ppm: 2.07 (s, 2H, NH_2, aliphatic alicyclic), 2.50-2.51 (m, 1H, CH, aliphatic alicyclic), 3.46-3.50 (m, 1H, CH, aliphatic alicyclic), 5.34 (s, 1H, NH-Ar), 6.99-7.01 (t, 1H *J*=8 Hz, Ar-H), 7.17-7.19 (d, 1H *J*=8 Hz, Ar-H), 7.23-7.27 (t, 1H *J*=4 Hz, Ar-H), 7.50-7.51 (d, 2H *J*=4 Hz, Ar-H), 7.82 (s, 1H, amide); ^{13}C NMR (100MHz, $CDCl_3$) δ ppm: 158.56 (C-amide), 143.20 (C-NH, Ar), 134.60 (Cl-C, Ar), 130.25 (CH, Ar), 123.51 (CH, Ar), 114.30 (CH, Ar), 78.35 (CH, aliphatic alicyclic), 40.25 (C-NH_2, aliphatic alicyclic); Elemental Analysis for $C_9H_8ClN_5O$: C, 45.49; H, 3.39; N, 29.47 (calculated): C, 45.50; H, 3.35; N, 29.45 (found).

3-Amino-4-(2-(4-chlorophenyl)hydrazono)-1*H*-pyrazol-5(4H)-one **10d**

Brown crystals: Yeild: 79 %; M.P.: 225-227 □C; FTIR υ_{max} (in cm^{-1}): 3313.71 (Primary -NH stretching), 3172.90 (Secondary -NH stretching), 1649.14 (-C=O stretching),1587.42 (Primary -NH bending), 1489.05-1444.68 (Secondary -NH bending), 1396.46-1265.30 (-C=C- stretching, Ar), 1109.07 (-C-N stretching), 1008.77 (-C-Cl stretching), 871.82-594.08 (-C-H bending, Ar); ^{1}H NMR (400MHz, $CDCl_3$-d_6, TMS) δ ppm: 1.05-1.09 (m, 1H, CH, aliphatic alicyclic), 1.20 (s, 2H, NH_2, aliphatic), 2.50-2.51 (m, 1H, CH, aliphatic alicyclic), 3.30-3.49 (m 1H, CH, aliphatic alicyclic), 5.51 (s, 1H, NH, Ar), 7.04-7.08 (d, 1H *J*=16 Hz, Ar-H), 7.24 (s, 1H, Ar-H), 7.30-7.34 (t, 1H J=16 Hz, Ar-H), 7.40-7.42 (d, 1H J=8 Hz, Ar-H), 8.05 (s, 1H, amide); ^{13}C NMR (100MHz, $CDCl_3$) δ ppm: 158.86

View Article Online
DOI: 10.1039/C3RA41604F

(C, amide), 149.65 (C-NH, Ar), 141.55 (C-Cl, Ar), 129.12 (CH, Ar), 123.98 (CH, Ar), 123.40 (CH, Ar), 114.75 (CH, Ar), 78.85 (C, aliphatic, alicyclic), 40.21 (C, aliphatic alicyclic): Elemental Analysis $C_9H_8ClN_5O$: C, 45.49; H, 3.39; N, 29.47 (calculated): C, 45.47; H, 3.36; N, 29.50 (found).

Method B: With Phenyl hydrazine

To a solution of appropriate hydrazone (**3a**,**b**; **4a**,**b** and **5a-d**) in glacial acetic acid (40 mL), phenyl hydrazine (0.012 mol) and anhydrous sodium acetate (0.01 mol) were added. The reaction mixture was then heated under reflux for 4 h. The resulting mixture was then poured into ice-cold water and stored in refrigerator overnight. The crude product, was washed with water, dried and recrystallized from ethanol.

3,5-Dimethyl-4-((4-nitrophenyl)diazenyl)-1-phenyl-4,5-dihydro-1*H*-pyrazole **6a**

Orange crystals; Yeild: 84 %; M.P.: 102-104 □C; FTIR υ_{max} (in cm^{-1}): 3100.64 (Secondary -NH stretching), 2924.09 (-C-H stretching, $-CH_3$), 1670.35 (-C=O stretching), 1597.08(Asymmetrical, $-NO_2$ stretching), 1548.84-1386.82 (-C=C- stretching, Ar), 1455, 1445 (N=N) 1330.88 (Symmetrical, $-NO_2$ stretching), 1235.96 (Secondary -NH bending), 1193.94 (-C-N stretching), 1022.27-682.80 (-C-H bending, Ar); ^{1}H NMR (400MHz, $CDCl_3$-d_6, TMS) δ ppm: 1.21 (s, 3H, CH_3), 2.48-2.49 (d, 1H *J*=4 Hz, CH, aliphatic alicyclic), 2.50-2.51 (d, 1H *J*=4 Hz, CH, aliphatic alicyclic), 2.63-2.64 (d, 3H *J*=4 Hz, CH_3), 7.41-7.44 (m, 1H, Ar-H), 7.50-7.52 (d, 1H *J*=8 Hz, Ar-H), 7.85-7.86 (d, 1H *J*=4 Hz, Ar-H), 7.88-7.89 (d, 1H *J*=4 Hz, Ar-H), 8.02 (s, 1H, Ar-H), 8.26-8.27 (d, 1H *J*=4 Hz, Ar-H); ^{13}C NMR (100MHz, $CDCl_3$) δ ppm: 156.38 (C, imine), 147.11 (C, imine, imidazole), 142.83 (C-NO_2, Ar), 141.10 (C-imidazole, Ar), 138.30 (CH, Ar), 136.25 (CH, Ar), 128.98 (CH, Ar), 128 (CH, Ar), 124.39 (CH, Ar), 122.10 (CH, Ar), 78.78 ($(CH_3)_2$-N, imidazole), 40.25 (C-CH_3, imidazole), 13.95 (CH_3), 10.95 (CH_3); Elemental Analysis for $C_{17}H_{17}N_5O_2$: C, 63.15; H, 5.30; N, 21.66 (calculated): C, 63.10; H, 5.32; N, 21.68 (found).

View Article Online
DOI: 10.1039/C3RA41604F

4-((4-Bromophenyl)diazenyl)-3,5-dimethyl-1-phenyl-4,5-dihydro-1*H*-pyrazole **6b**

Yellowish crystals; Yeild: 80 %; M.P.: 110-112 □C; FTIR υ_{max} (in cm^{-1}): 3045.60-2958.80 (-C-H stretching, -CH_3), 1662.64 (-C=O stretching), 1598.99-1506.41 (-C=C- stretching, Ar), 1455, 1445 (N=N), 1114.86 (-C-Br stretching), 1064.71-522.71 (-C-H bending, Ar); ^{1}H NMR (400MHz, $CDCl_3$-d_6, TMS) δ ppm: 0.92 (s, 3H, CH_3), 1.24-1.25 (d 3H *J*=4 Hz, CH_3), 2.60 (m 1H, CH, aliphatic alicyclic), 2.64-2.65 (d, 1H *J*=4 Hz, CH, aliphatic alicyclic), 7.51-7.52 (t, 1H *J*=4 Hz, Ar-H), 7.59-7.60 (d, 1H *J*=4 Hz, Ar-H), 7.61-7.62 (t, 1H *J*=4 Hz, Ar-H), 7.70 (m, 1H, Ar-H), 7.71-7.72 (d, 1H *J*=4 Hz, Ar-H); ^{13}C NMR (100MHz, $CDCl_3$) δ ppm: 152.36 (N=C-CH_3, imine, aliphatic alicyclic), 143.92 (C-N, Ar), 139.49 ($(CH_3)_2$-N, Ar), 136.20 (CH, Ar), 132.11 (CH, Ar), 129.28 (CH, Ar), 128.17 (CH, Ar), 124.88 (CH, Ar), 123.54 (C-Br, Ar), 77.36 (C-$(CH_3)_2$, aliphatic alicyclic), 76.78 $(CH_3)_2$-CH_3, aliphatic alicyclic), 14.16 (CH_3), 11.39 (CH_3); Elemental Analysis for $C_{17}H_{17}BrN_4$: C, 57.15; H, 4.80; N, 15.68 (calculated); C, 57.13; H, 4.83; N, 15.65 (found).

3-Methyl-4-(2-(4-nitrophenyl)hydrazono)-1-phenyl-1*H*-pyrazol-5(4*H*)-one **9a**

Reddish-orange crystals; Yeild: 88 %; M.P.: 181-183 □C; FTIR υ_{max} (in cm^{-1}): 3107.32 (Secondary -NH stretching), 1662.64 (-C=O stretching), 1560.41 (-NH bending), 1527.62 (Asymmetrical, -NO_2 stretching), 1490.97 (Symmetrical, -NO_2 stretching), 1330.88 (-C=C- stretching, Ar), 1236.37 (-C-N stretching), 1147.65-570.93 (-C-H bending, Ar); ^{1}H NMR (400MHz, $CDCl_3$-d_6, TMS) δ ppm: 1.88-1.89 (d, 3H *J*=4 Hz, CH_3), 2.31 (m, 1H, CH, aliphatic), 2.50-2.51 (m, 1H, CH, aliphatic), 3.29 (s, 1H, NH, Ar), 7.13-7.17 (t, 1H *J*=16 Hz, Ar-H), 7.35-7.40 (m, 1H, Ar-H), 7.59-7.63(t, 1H *J*=16 Hz, Ar-H), 7.87-7.90 (d, 1H *J*=12 Hz, Ar-H), 7.93-7.96 (d, 1H *J*=12 Hz, Ar-H); ^{13}C NMR (100MHz, $CDCl_3$) δ ppm: 156.18 (C-amide), 148.58 (C-NH, Ar), 142 (C-N$(CH_3)_2$, Ar), 128.57 (CH, Ar), 124.64 (CH, Ar), 121.82(CH, Ar), 119 (CH, Ar), 117.65 (CH, Ar),110.50 (CH, Ar), 78.79 ($(CH_3)_2$C-N, aliphatic), 11.55 (CH_3); Elemental Analysis for $C_{16}H_{13}N_5O_3$: C, 59.44; H, 4.05; N, 21.66 (calculated); C, 59.42;

View Article Online
DOI: 10.1039/C3RA41604F

H, 4.09; N, 21.70 (found).

4-(2-(4-Bromophenyl)hydrazono)-3-methyl-1-phenyl-1*H*-pyrazol-5(4*H*)-one **9b**

Bright-orange crystals; Yeild: 76 %; M.P.: 145-147 □C; FTIR υ_{max} (in cm^{-1}): 3211.48 (Secondary -NH stretching), 1666.50 (-C=O stretching), 1587.42-1564.27 (-NH bending), 1483.26-1375.25 (-C=C- stretching, Ar), 1249.87 (-C-N stretching), 1055.06 (-C-Br stretching), 968.27-594.08 (-C-H bending, Ar); ^{1}H NMR (400MHz, $CDCl_3$-d_6, TMS) δ ppm: 1.18 (d, 3H *J*=4 Hz, CH_3), 2.23 (s, 1H, NH, Ar), 2.51 (m, 1H, CH, aliphatic alicyclic), 7.08-7.12 (t, 1H *J*=16 Hz, Ar-H), 7.27-7.34 (m, 1H, Ar-H), 7.41-7.44(d, 1H, *J*=9 Hz, Ar-H), 7.68 (s, 1H, Ar-H), 7.84-7.86 (d, 1H *J*=8 Hz, Ar-H); ^{13}C NMR (100MHz, $CDCl_3$) δ ppm: 156.83 (C-amide), 147.91 (C-NH, Ar), 139.99 (CH, Ar), 137.56 (CH, Ar), 132.01 (CH, Ar), 128.37 (CH, Ar), 124.51 (CH, Ar), 117.73 (CH, Ar), 117.04 (CH, Ar), 78.06 (CH, aliphatic), 40.26 (CH, aliphatic), 11.32 (CH_3, aliphatic); Elemental Analysis for $C_{16}H_{13}BrN_4O$: C, 53.80; H, 3.67; N, 15.68 (calculated); C, 53.83; H, 3.65; N, 15.66 (found).

3-Amino-4-(2-(4-nitrophenyl)hydrazono)-1-phenyl-1*H*-pyrazol-5(4*H*)-one **11a**

Pale-yellow crystals; Yeild: 72%; M.P.: 85-87 □C; FTIR υ_{max} (in cm^{-1}): 3385.07-3325.28 (Primary -NH stretching), 3186.40 (Secondary -NH stretching), 1683.86 (-C=O stretching), 1637.56 (Primary -NH bending), 1600.92 (Secondary -NH bending), 1481.33(Asymmetrical, -NO_2 stretching), 1404.18 (Symmetrical, -NO_2 stretching), 1253.73 1249.87-1207.44 (-C=C- stretching, Ar), 1114.86 (-C-N stretching), 999.13-580.57 (-C-H bending, Ar); ^{1}H NMR (400MHz, $CDCl_3$-d_6, TMS) δ ppm: 1.29-1.36 (m, 1H, CH, aliphatic alicyclic), 1.89 (s, 2H, NH_2, aliphatic alicyclic), 2.50-2.51 (m, 1H, CH, aliphatic alicyclic), 3.11 (s, 1H, NH, Ar), 7.45-7.54 (m, 1H, Ar-H), 7.75-7.77 (d, 2H *J*=8 Hz, Ar-H), 7.78-7.80 (d, 2H *J*=8 Hz, Ar-H), 7.82-7.83 (d, 1H *J*=4 Hz, Ar-H), 7.84-7.85 (d, 1H *J*=4 Hz, Ar-H), 7.89-7.92 (d, 1H *J*=12 Hz, Ar-H); ^{13}C NMR (100MHz, $CDCl_3$) δ ppm: 160.45 (C-amide), 148.47 (C-NH, Ar), 143.18 ((CH_3)$_2$-N-C, Ar), 142.06 (NO_2-C, Ar), 130.14 (CH, Ar), 129.83 (CH, Ar), 121.58 (CH, Ar),

View Article Online
DOI: 10.1039/C3RA41604F

119.22 (CH, Ar), 118.29 (CH, Ar), 114.42 (CH, Ar), 110.83 (CH, Ar), 78.07 (CH, aliphatic alicyclic), 62.11 (CH, aliphatic alicyclic); Elemental Analysis for $C_{15}H_{12}N_6O_3$: C, 55.55; H, 3.73; N, 25.91 (calculated); C, 55.53; H, 3.70; N, 25.94 (found).

3-Amino-4-(2-(4-bromophenyl)hydrazono)-1-phenyl-1*H*-pyrazol-5(4*H*)-one **11b**

Pale-yellow crystals; Yeild: 82%; M.P.: 130-132 □C; FTIR υ_{max} (in cm^{-1}): 3217.27 (Primary -NH stretching), 3198.02 (Secondary -NH stretching), 1687.71 (-C=O stretching), 1600.92 (Primary -NH bending), 1535.43 (Secondary -NH bending), 1479.40-1377.17 (-C=C- stretching, Ar), 1328.95-1263.37(-C-N stretching), 1132.21 (-C-Br stretching), 1068.56-576.72 (-C-H bending, Ar); ^{1}H NMR (400MHz, $CDCl_3$-d_6, TMS) δ ppm: 1.89-1.91 (d, 3H *J*=8 Hz, CH_3), 2.50-2.52 (m, 1H, CH, aliphatic), 3.26 (s, 1H, NH, Ar-H), 4.24-4.33 (m, 1H, CH, aliphatic), 7.32-7.46 (m, 1H, Ar-H), 7.93 (s, 1H, amide); ^{13}C NMR (100MHz, $CDCl_3$) δ ppm: 160.83 (C-amide), 141.46 (C-NH, Ar), 131.67 (C-NO_2, Ar), 117.62 (CH, Ar), 111.20 (CH, Ar), 78.61 (CH, aliphatic), 39.60 (CH, aliphatic), 13.96 (CH_3); Elemental Analysis for $C_{15}H_{12}BrN_5O$: C, 50.30; H, 3.38; N, 19.55 (calculated); C, 50.33; H, 3.35; N, 19.50

3-Amino-4-(2-(3-Chlorophenyl)hydrazono)-1-phenyl-1*H*-pyrazol-5(4*H*)-one **11c**

Light-yellow crystals; Yeild: 86%; M.P.: 160-162 C; FTIR υ_{max} (in cm^{-1}): 3228.84 (Primary -NH stretching), 3082.25 (Secondary -NH stretching), 1699.29 (-C=O stretching), 1602.85-1558.48 (Primary -NH bending), 1498.69-1460.11 (Secondary -NH bending), 1371.39-1328.95 (-C=C- stretching, Ar), 1251.80 (-C-N stretching), 1112.93 (-C-Cl stretching), 1018.41-586.36 (-C-H bending, Ar); ^{1}H NMR (400MHz, $CDCl_3$-d_6, TMS) δ ppm: 1.29-1.35 (m, 1H, CH, aliphatic alicyclic), 1.92 (s, 2H, NH_2, aliphatic alicyclic), 2.51 (m, 1H, CH, aliphatic alicyclic), 3.20 (s, 1H, C-NH, Ar), 4.25-4.33 (m, 1H, CH, aliphatic alicyclic), 7.00-7.02 (d, 1H *J*=8 Hz, Ar-H), 7.06-7.09 (m , 1H, Ar-H), 7.20-7.30 (m, 1H, Ar-H), 7.36-7.38 (d, 1H *J*=8 Hz, Ar-H), 7.41 (s, 1H, Ar-H), 7.46 (s, 1H, Ar-H); ^{13}C NMR

View Article Online
DOI: 10.1039/C3RA41604F

(100MHz, $CDCl_3$) δ ppm: 160.82 (C-amide), 143.08 (C-NH, Ar), 141.95 ($(CH_3)_2$-N, Ar), 134.54 (Cl-C, Ar), 130.35 (CH, Ar), 124.04 (CH, Ar), 115.85 (CH, Ar), 114.67 (CH, Ar), 110.82 (CH, Ar), 104.97 (CH, Ar), 104.53 (CH, Ar), 78.31 (CH, aliphatic alicyclic), 61.93 (CH, aliphatic alicyclic); Elemental Analysis for : C, 57.42; H, 3.86; Cl, 11.30; N, 22.32; Elemental Analysis for $C_{15}H_{12}ClN_5O$: C, 57.42; H, 3.86; N, 22.32 (calculated); C, 57.45; H, 3.87; N, 22.34 (found)

3-Amino-4-(2-(3-chlorophenyl)hydrazono)-1-phenyl-1*H*-pyrazol-5(4*H*)-one **11d**

Dark-green crystals; Yeild: 82%; M.P.: 210-212 □C; FTIR υ_{max} (in cm^{-1}): 3211.48 (Primary -NH stretching), 3163.26 (Secondary -NH stretching), 2980.02 (-C-H stretching, $-CH_3$), 1741.72 (-C=O stretching), 1687.71-1593.20 (Primary -NH bending), 1498.69 (Secondary -NH bending), 1373.32-1311.59 (-C=C- stretching, Ar), 1241.70 (-C-N stretching), 1109.93 (-C-Cl stretching), 1022.27-599.86 (-C-H bending, Ar); ^{1}H NMR (400MHz, $CDCl_3$-d_6, TMS) δ ppm: 1.30-135 (m, 1H, CH, aliphatic alicyclic), 1.92 (s, 2H, NH_2, aliphatic alicyclic), 2.50-2.51 (m, 1H, CH, aliphatic alicyclic), 3.29 (s 1H, NH, Ar), 4.25-4.33 (m, 1H, CH, aliphatic alicyclic), 7.06-7.10 (t, 1H *J*=16 Hz, Ar-H), 7.12-7.16 (t, 1H *J*=16 Hz, Ar-H), 7.28-7.41 (m, 1H, Ar-H), 7.46-7.48 (d, 1H J=8 Hz, Ar-H), 7.99 (s, 1H, Ar-H); ^{13}C NMR (100MHz, $CDCl_3$) δ ppm: 161.11 (C, amide), 141.80 (C-NH, Ar), 140.75 (C-NH, Ar), 129.18 (C-Cl, Ar), 128.89 (CH, Ar), 125.45 (CH, Ar), 124.53 (CH, Ar), 116.04 (CH, Ar), 115.76 (CH, Ar), 115.13 (CH, Ar), 111.15 (CH, Ar), 103.88 (CH, Ar), 103.40 (CH, Ar), 78.72 (C, aliphatic, alicyclic), 61.72 (C, aliphatic alicyclic); Elemental Analysis for : C, 57.42; H, 3.86; N, 22.32 (calculated); C, 57.44; H, 3.85; N, 22.35 (found).

Method C: With Urea

A mixture of hydrazono derivative (**3a,b**; 0.005 mol) and urea (0.01 mol) in ethanol (50 mL) was heated under reflux for 5 h. After cooling to room temperature, crushed ice was added and the mixture was stirred for 1 h. The separated product was collected by filtration and recrystallized from ethanol.

View Article Online
DOI: 10.1039/C3RA41604F

4,6-dimethyl-5-(2-(4-nitrophenyl)hydrazono)pyrimidin-2(5*H*)-one **7a**

Light-yellow crystals; Yeild: 78%; M.P.: 165-166 □C; FTIR υ_{max} (in cm^{-1}): 3118.90 (Secondary -NH stretching), 1680.00 (-C=O stretching), 1597.06(Asymmetrical, $-NO_2$ stretching), 1496.76 (Symmetrical, $-NO_2$ stretching), 1355.96 (Secondary -NH bending), 1311.12-1163.80 (-C=C- stretching, Ar), 1116.78 (-C-N stretching), 1049.28-611.43 (-C-H bending, Ar); ^{1}H NMR (400MHz, $CDCl_3$-d_6, TMS) δ ppm: 1.72 (s, 3H, CH_3), 1.91 (s, 3H, CH_3), 7.68-7.70 (d, 1H *J*=16 Hz, Ar-H), 8.11 (s, 1H, Ar-NH), 8.20-8.23 (d, 1H *J*=12 Hz, Ar-H); ^{13}C NMR (100MHz, $CDCl_3$) δ ppm: 196.80 (C, carbonyl), 195.12 (C, imine), 166.16 (C, imine), 139.65 (C-NH, Ar), 132.42 (C-NO_2, Ar), 131.42 (CH, Ar), 118.28 (CH, Ar), 116.95 (CH, Ar), 30.21 (CH_3), 12.12 (CH_3); Elemental Analysis for $C_{12}H_{11}N_5O_3$: C, 52.75; H, 4.06; N, 25.63 (calculated); C, 52.76; H, 4.02; N, 25.60 (found).

5-(2-(4-Bromophenyl)hydrazono)-4,6-dimethylpyrimidin-2(5*H*)-one **7b**

Dark-yellow crystals; Yeild: 88%; M.P.: 90-92 □C; FTIR υ_{max} (in cm^{-1}): 3072.60 (Secondary -NH stretching), 1666.50 (-C=O stretching), 1624.06-1413.82 (-C=C- stretching, Ar), 1375.25-1317.38 (-NH bending), 1187.79 (-C-N stretching), 1070.49 (-C-Br stretching), 929.69-507.39 (-C-H bending, Ar); ^{1}H NMR (400MHz, $CDCl_3$-d_6, TMS) δ ppm: 2.49 (s, 3H, CH_3), 2.61 (s, 3H, CH_3), 7.28 (s, 1H, N-NH, Ar), 7.29-7.31 (d, 1H *J*=8 Hz, Ar-H), 7.51-7.53 (d, 1H *J*=8 Hz, Ar-H); ^{13}C NMR (100MHz, $CDCl_3$) δ ppm: 198.20 (C-carbonyl), 196.90(C-imine), 166.10 (C-imine), 140.67(NH-C, Ar), 133.53 (CH, Ar), 132.69 (CH, Ar), 118.64 (CH, Ar), 117.65 (CH, Ar), 77.36 (C-Br, Ar), 31.69 (CH_3), 26.61 (CH_3); Elemental Analysis for $C_{12}H_{11}BrN_4O$: C, 46.93; H, 3.61; N, 18.24 (calculated); C, 46.93; H, 3.61; N, 18.24 (found).

Biological Activity

Anti-HIV activity

For anti-HIV screening of the compounds, TZM-*bl* cells (4×10^4/ well) were seeded in 24 well plates

View Article Online
DOI: 10.1039/C3RA41604F

and cultured overnight at 37 °C in 5% CO_2 incubator. In separate vials, HIV-1 NL4.3 at a concentration equivalent to 0.05 multiplicity of infection (MOI) with respect to seeded TZM-*bl* cells were treated with 50 µg mL^{-1} of different test compounds and vehicle control for 1 h at 37 °C. Subsequently, pre-treated viruses were added in duplicate to TZM-*bl* cells growing in 24 well plates and were incubated for 4 h at 37 °C. After incubation, the culture was removed and cells were washed with 50mM PBS followed by addition of fresh medium with 50 µg/mL test compounds. Cells were further cultured for 48 h in 5% CO_2 incubator at 37 °C. AZT was added as positive control, whereas, negative control comprised cells with untreated virus. After incubation, cells were washed with PBS and lysed using Promega Lysis Buffer (1X) followed by centrifugation. The results were expressed as percentage inhibition.

Cytotoxicity assay

MTT test was used to assess the cytotoxicity of the compounds based on the capacity for viable cells to metabolize a tetrazolinium colorless salt to a blue formazan in mitochondria. In brief, TZM-*bl* cells were seeded in 96 well tissue culture plates (6000 cells/well) and incubated in 5% CO_2 incubator at 37 °C for 24 h. Following incubation cells were treated with varying concentration of the test compounds for 48 h at 37 °C. Appropriate solvent was added as negative control. After incubation 20 µL of MTT reagent (5mg/mL in 50 mM PBS) was added to the wells and the culture plate was left for further incubation at 37 °C for 4 h. After incubation, cells were cleaned off the spent medium and 120 µL of MTT solvent [20% SDS and 50% dimethyl formamide (DMF) in 50 mM of PBS] was added to each well and culture plate was left for an overnight incubation at 37 °C. The absorbance was taken at 570 nm with 690 nm reference filter using ELISA reader. Percent viability was calculated by absorbance of the test sample treated cells divided by absorbance of untreated cells multiplied by hundred.

Molecular docking

A Non-nucleoside RT Inhibitor TMC278 (Rilpivirine) docked into the Crystal Structure of HIV-1 Reverse Transcriptase (RT) (3m8p:pdb) was used as starting model for this study. The protein was

View Article Online
DOI: 10.1039/C3RA41604F

prepared, docked, scored, and the molecular dynamics simulation carried out using standard procedures. All computational analysis were carried out using Discovery Studio 2.5 (Accelrys Software Inc., San Diego; http://www.accelrys.com).

Preparation of receptor

The target protein that complexed with TMC278 (Rilpivirine) was taken, the ligand TMC278 (Rilpivirine) extracted, and the bond order were corrected. The hydrogen atoms were added, and their positions were optimized using the all-atom CHARMm (version c32b1) forcefield with Adopted Basis set Newton Raphson (ABNR) minimization algorithm, until the root mean square (r.m.s) gradient for potential energy was <0.05 kcal mol^{-1} $Å^{-1}$. Using the 'Binding Site' tool panel available in DS 2.5, the minimized crystal Structure of HIV-1 Reverse Transcriptase (RT) was defined as receptor. The receptor having defined binding site was used for the docking studies.

Ligand setup

Using the built-and-edit module of DS 2.5, various ligands were and built all-atom CHARMm forcefield parameterization was assigned, and minimized using the ABNR method. A conformational search of the ligand was carried out using a stimulated annealing molecular dynamics (MD) approach. The ligand was heated to a temperature of 700 K and then annealed to 200 K. Thirty such cycles were carried out. The transformation obtained at the end of each cycle was further subjected to local energy minimization, using the ABNR method. The 30 energy-minimized structures were then superimposed and the lowest energy conformation occurring in the major cluster was taken to be the most probable conformation.

Docking and Scoring

LigandFit protocol of DS 2.5 was used for the docking of ligands with HIV-1 RT protein structure (pdb id: 3m8p) [24]. The LigandFit docking algorithm combines a shape comparison filter with a

View Article Online
DOI: 10.1039/C3RA41604F

Monte Carlo conformational search to generate docked poses consistent with the binding site shape. These initial poses are further refined by rigid body minimization of the ligand with respect to the grid based calculated interaction energy using the Dreiding forcefield [25]. The receptor protein conformation was kept fixed during docking, and the docked poses were further minimized using all-atom CHARMm (version c32b1) forcefield and smart minimization method (steepest descent followed by conjugate gradient), until r.m.s gradient for potential energy was <0.05 kcal mol^{-1} $Å^{-1}$. The atoms of ligand and the side chains of the residues of the receptor within 5 Å from the center of the binding site were kept flexible during minimization. The docked conformation of the molecules was then scored on the basis of scoring parameter and has been already given in result and discussion section. Furthermore, to assess the binding affinity of ligands for receptor by binding energies was calculated by employing highest stable ligand-receptor complex through the protocol 'Calculate Binding Energies' within DS 2.5 using the default settings.

Antibacterial Screening (Minimum inhibitory concentration)

All synthesized compounds were screened for their minimum inhibitory concentration (MIC, μg/mL) against selected four Gram-positive, *viz. Staphylococcus aureus* (NCIM-2079), *Bacillus subtilis* (NCIM-2063), *Bacillus cereus* (NCIM-2156), *Staphylococcus Epidermidis* and four Gram-negative bacterial strains *viz. Pseudomonas aeruginosa* (NCIM-2036), *Escherichia coli* (NCIM-2065), *Proteus Mirabilis* and *Proteus vulgaris* by the broth dilution method as recommended by the National Committee for Clinical Laboratory Standards with minor modifications [26]. Cefixime was used as standard antibacterial agent. Solutions of the test compounds and reference drug were prepared in dimethyl sulfoxide (DMSO) at concentrations of 100, 50, 25, 12.5, 6.25, 3.125 and 1.56 μg/mL. Nine tubes were prepared in duplicate with the second set being used as MIC reference controls (16–24 h visual). After sample preparation, the controls were placed in a 37 □C incubator and read for macroscopic growth (clear or turbid) the next day. Into each tube, 0.8 mL of nutrient broth was

View Article Online
DOI: 10.1039/C3RA41604F

pipetted (tubes 2–8); tube 1 (negative control) received 1.0 mL of nutrient broth and tube 9 (positive control) received 0.9 mL of nutrient. Tube 1, the negative control, did not contain bacteria or antibiotic. The positive control, tube 9, received 0.9 mL of nutrient broth because it contained bacteria but not antibiotic. The test compounds were dissolved in DMSO (100 μg/mL); 0.1 mL of increasing concentration of the prepared test compounds is serially diluted from tube 2 to tube 7 from highest (100 μg mL^{-1}) to lowest (1.56 μg mL^{-1}) concentration (tubes 2–8 containing 100, 50, 25, 12.5, 6.25, 3.125 and 1.56 μg mL^{-1}). After this process, each tube was inoculated with 0.1 mL of the bacterial suspension whose concentration corresponded to 0.5 McFarland scale (9×10^8 cells/mL), and each bacterium was incubated at 37 □C for 24 h at 150 rpm. The final volume in each tube was 1.0 mL. The incubation chamber was kept humid. At the end of the incubation period, MIC values were recorded as the lowest concentration of the substance that gave no visible turbidity, that is, no growth of inoculated bacteria.

Conclusions

As a concluding remark, we have developed a novel series of compounds with potent anti-HIV and antibacterial activity along with optimal physico-chemical parameters. It was confirmed that designed molecules have the possibility of introducing the chemical diversity around the core skeleton to generate newer potent molecules. Our efforts are going in this field and will be reported subsequently in future.

Acknowledgement:

Authors are thankful to Punjab University, Chandigarh, India, and SHIATS, India for providing the Instrumental and Infrastructural facilities, respectively.

View Article Online
DOI: 10.1039/C3RA41604F

Notes and references

[a] *Department of Pharmaceutical Sciences, Sam Higginbottom Institute of Agriculture, Technology & Sciences, Allahabad 211007, India. Email: udaysingh98@gmail.com*

[b] *Anand College of Pharmacy, Agra 282007, India*

[c] *National Institute of Immunology, Aruna Asaf Ali Marg, New Delhi 110067, India*

[d] *Nucleic Acids and Antiviral Research Laboratory, Department of Chemistry, University of Allahabad, Allahabad 211002, India. Email: singhramk@rediffmail.com*

1. P. M. Sharp and B. H. Hahn, *Philos. Trans. R. Soc. Lond. B Biol. Sci.* 2010, **365**, 2487.
2. World AIDS Day Report, UNAIDS, 2012.
3. P.A. Volberding, S.W. Lagakos, J.M. Grimes, D.S. Stein, H.H. Balfour Jr, R.C. Reichman, J.A. Bartlett, M.S. Hirsch, J.P. Phair, R.T. Mitsuyasu, et al. *JAMA*. 1994, **272**, 437.
4. F. S. Pedersan and M. Duch, Retroviral Replication, In: eLS. 2001 Nature Publishing Group, http://www.els.net/.
5. D. Harris, R. Lee, H.S. Misra, P.K. Pandey and V.N. Pandey, *Biochemistry*, 1998, **37**, 5903.
6. D. Li , P. Zhan , E. De Clercq and X. Liu, *J. Med. Chem.* 2012, **55**, 3595.
7. F. Esposito, A. Corona and E. Tramontano, *Mol. Biol. Int.* 2012, ID 586401, 23 pages, doi:10.1155/2012/586401.
8. P. Zhan, X. Chen, D. Li, Z. Fang, E. De Clercq and X. Liu, *Med. Res. Rev.* 2013, **33**, 1-72.
9. (a) L.A. Kohlstaedt, J. Wang, J.M. Friedman, P.A. Rice and T.A. Steitz, *Science*, 1992, **256**, 1783. (b) J. Ding, K. Das, C. Tantillo, W. Zhang, A.D. Clark Jr., S. Jessen, X. Lu, Y. Hsiou, A. Jacobo-Monlina, K. Andries, R. Pauwels, H. Moereels, L. Koymans, P.A.J. Janssen, R. Smith, M.K. Koepke, C. Michejda, S.H. Hughes and E. Arnold, *Structure*, 1995, **3**, 365.
10. S.S. Abdool Karim , G.J. Churchyard , Q.A. Karim and S.D. Lawn, Lancet, 2009, 374, 921.
11. (a) C.E. Mowbray, C. Burt, R. Corbau, S. Gayton, M. Hawes, M. Perros, I. Tran, D.A. Price, F.J. Quinton, M.D. Selby, P.A. Stupple, R. Webster and A. Wood, *Bioorg. Med. Chem. Lett.*

View Article Online
DOI: 10.1039/C3RA41604F

2009, **19**, 5857. (b) H. Azijn, I. Tirry, J. Vingerhoets, M.P. de Béthune, G. Kraus, K. Boven, D. Jochmans, E. Van Craenenbroeck, G. Picchio and L.T. Rimsky, *Antimicrob. Agents Chemother.* 2010, **54**, 718. (c) D.M. Himmel, S.G. Sarafianos, S. Dharmasena, M.M. Hossain, K. McCoy-Simandle, T. Ilina, A.D. Clark Jr, J.L. Knight, J.G. Julias, P.K. Clark, K. Krogh-Jespersen, R.M. Levy, S.H. Hughes, M.A. Parniak and E. Arnold, *ACS Chem. Biol.* 2006, **1**, 702.

12. (a) S. Lupsor, F. Aonofriesei and M. Iovu, *Med. Chem. Res.* 2012, **21**, 3035. (b) R.B. Patel, P.S. Desai, K.R. Desai and K. Chikhalia, *Indian J. Chem.* 2006, **45B**, 773. (c) J .Wu, S. Kang, B. Song, D. Hu, M. He, L. Jin and S. Yang, *Chem. Cent. J.* 2012, **6**, 28.
13. (a) R. K. Singh, D. Yadav, D. Rai, G. Kumari, C. Pannecouque, E. De Clercq, *Eur. J. Med. Chem.* 2010, **45**, 3787. (b) R. K. Singh, D. Rai, D. Yadav, A. Bhargava, J. Balzarini, E. De Clercq, *Eur. J. Med. Chem.* 2010, **45**,1078. (c) G. Kumari , Nutan, M. Modi, S. K. Gupta, R. K. Singh, *Eur. J. Med. Chem.* 2011, **46**, 1181.
14. J.L. Jones, D.L. Hanson, M.S. Dworkin, et al. MMWR CDC Surveill Summ. 1999, 48, 1.
15. (a) www.molinspiration.com, (b) C. A. Lipinski, F. Lombardo, B. W. Dominy and P. J. Feeney, *Adv. Drug. Delivery Rev.* 1997, **23**, 4. (c) U. P. Singh and R. K. Singh, *Retrovirology* 2011, **8**(Suppl 2), P82
16. P. Ertl, B. Rohde and P. Selzer, *J.Med.Chem.* 2000, **43**, 3714.
17. D. F. Veber, S. R. Johnson, H. -Y. Cheng, B. R. Smith, K. W. Ward and K. D. Kopple, *J. Med. Chem.* 2002, **45**, 2615.
18. G. La Regina, A. Coluccia and R. Silvestri, *Antivir. Chem. Chemother.* 2010, **20**, 213.
19. A Nicholls, K.A. Sharp and B. Honig, *Proteins*, 1991, **11**, 281.
20. D.K. Gehlhaar, G.M. Verkhivker, P.A. Rejto, C.J. Sherman, D.B. Fogel, L.J.Fogel and S.T. Freer, *Chem. Biol.* 1995, **2**, 317.

View Article Online
DOI: 10.1039/C3RA41604F

21. D.K. Gehlhaar, D.Bouzida and P.A. Rejto, Rational drug design: novel methodology and practical applications. In: L. Parrill, M. Rami Reddy, editors. Washington, DC: American Chemical Society; 1999. pp. 292–311.pp. 719 (ACS symposium series).

22. I. Muegge and Y.C. Martin, *J. Med. Chem.* 1999, **42**, 791.

23. D.B. Kitchen, H. Decornez, J.R. Furr, J. Bajorath. *Nat. Rev. Drug Discov.* 2004 **3**, 935.

24. C. M. Venkatachalam, X. Jiang, T. Oldfield and M. Waldman, *J. Mol. Graph. Model.* 2003, **21**, 289.

25. S. L. Mayo, B. D. Olafson and W. A. III Goddard, *J. Phys. Chem.* 1990, **94**, 8897.

26. National Committee for Clinical Laboratory Standards, Standard Methods for Dilution Antimicrobial Susceptibility Test for Bacteria Which Grow Aerobically, Villanova, NCCLS, 1982, p. 242.

Phenyl hydrazone bearing pyrazole and pyrimidine scaffolds: Design and discovery of novel class of Non-Nucleoside Reverse Transcriptase Inhibitors (NNRTIs) against HIV-1 and their antibacterial properties

Udaya Pratap Singh,*[a,d] Hans Raj Bhat,[a] Amita Verma,[a] Mukesh Kumar Kumawat,[b] Rajinder Kaur, [c] S. K. Gupta [c] and Ramendra K. Singh*[d]

Graphical Abstract:

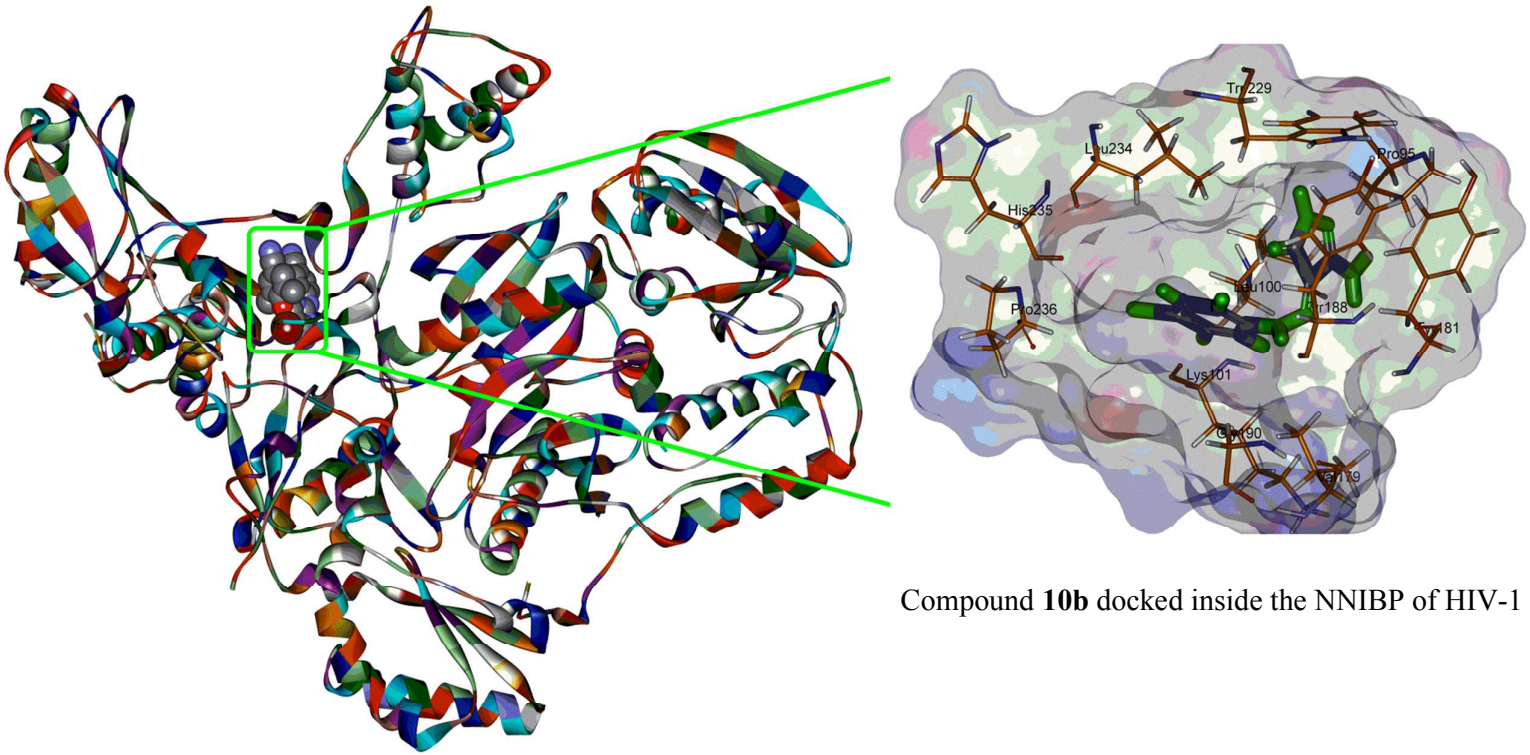

Compound **10b** docked inside the NNIBP of HIV-1 RT

- Phenyl hydrazone bearing pyrazole and pyrimidine scaffolds have been shown as potential anti-HIV agents with antibacterial properties.